CHAPTER ONE HUNDRED FOURTEEN

The Computation of Bed Shear in a Numerical Model

W. Leeuwenstein[*] and H.G. Wind[**]

1. Introduction

Obstructions located in coastal and offshore waters usually dis-
turb the natural flow pattern. This disturbed flow will, in general,
cause local morphological changes in the position of the erodable
boundary.
    Often these changes should not be allowed to exceed certain
limits, for example, when local scour around an offshore construction
may endanger foundations.
    Local morphological changes result from changes in the local
sediment balance, brought about by the flow disturbance.

In the present paper a mathematical model is described which
gives the bottom shear stresses and the configuration of the seabed
around an obstruction using a computation of the two dimensional tur-
bulent flow field. The obstruction considered is a submarine pipeline
laid uncovered on a seabed consisting of non-cohesive sediment. A
research project on the local scour near submarine pipelines is being
carried out at the Delft University of Technology. Part of the project
is the application and extension of an advanced numerical flow model
for scour development near pipelines on the seabed exposed to current
action. This work is being carried out in cooperation with the Delft
Hydraulics Laboratory. The code of the flow model has been developed
in a joint venture between the Delft Hydraulics Laboratory and the
Laboratoire National d"Hydraulique in France.

The turbulent flow field is computed taking into account the
influence of turbulence generated at the bed and by the pipe. The bed
shear stresses are assumed to play the key role in the interaction
between the flow and the seabed. In the computer model the bed shear
is related to the flow through the "law of the wall". The model opera-
tion is schematized in the diagram below in which the first loop re-
presents the evolution of the velocity field through a series of
hydraulic time steps. After the velocity field is stabilized, in the
second loop one morphological time step can be used for the computa-
tion of the local seabed changes. In this second loop the computed bed
shear is applied together with a sediment transport formula.

After the morphological time step a new bed topography is ob-
tained and a new grid is generated for the next flow computation.

---

[*]   Delft University of Technology, The Netherlands
[**] Delft Hydraulics Laboratory, The Netherlands
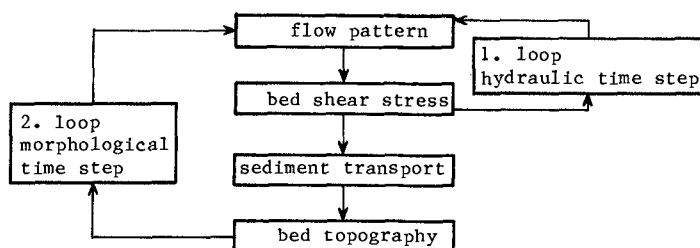
Fig. 1   Flow diagram of model operation

2.   Theory

2.1   Flow Field

A detailed computation of the flow pattern is a prerequisite for
the calculation of small scale changes of the seabed. In the present
example the changes in the seabed are of the same magnitude as the
pipe diameter which is, in general, small relative to the flow depth.
    The basic equations describing the flow are the equations of
motion and continuity for the fluid. The two dimensional unsteady
Navier-Stokes equations for the mean flow are written as:

$$\frac{\partial u}{\partial t} + u \frac{\partial u}{\partial x} + v \frac{\partial u}{\partial y} + \frac{1}{\rho} \frac{\partial p}{\partial x} - \frac{1}{\rho} \left(\frac{\partial \tau_{xy}}{\partial y} + \frac{\partial \sigma_{xx}}{\partial x} \right) = 0$$

$$\frac{\partial v}{\partial t} + u \frac{\partial v}{\partial x} + v \frac{\partial v}{\partial y} + \frac{1}{\rho} \frac{\partial p}{\partial y} - \frac{1}{\rho} \left(\frac{\partial \tau_{xy}}{\partial x} + \frac{\partial \sigma_{yy}}{\partial y} \right) = 0 \qquad (1)$$

where u and v are the horizontal (x) and vertical (y) velocity compo-
nents respectively, p is the pressure and σ_{xx}, σ_{yy}, τ_{xy} are the shear
stresses in the fluid, ρ is the density of the fluid.
The equation of continuity is:

$$\frac{\partial u}{\partial x} + \frac{\partial v}{\partial y} = 0 \qquad (2)$$

In the equations of motion the viscous and turbulent shear
stresses appear together as

$$\sigma_{xx} = \rho \, \nu \, 2 \frac{\partial u}{\partial x} - \rho \, \overline{u'^2}$$

$$\tau_{xy} = \rho \, \nu \, \left(\frac{\partial u}{\partial y} + \frac{\partial v}{\partial x} \right) - \overline{\rho u' v'} \qquad (3)$$

$$\sigma_{yy} = \rho \, \nu \, 2 \frac{\partial v}{\partial y} - \rho \, \overline{v'^2}$$

where ν is the kinematic viscosity of the fluid, u' and v' are the
turbulent fluctuations associated with the time-averaged velocities u
and v respectively.

Using Boussinesq's hypothesis the turbulent stresses in Eq. (3)
can be written as:

$$-\overline{u'v'} = \nu_t \left(\frac{\partial u}{\partial y} + \frac{\partial v}{\partial x}\right) \tag{4}$$

where ν_t is the turbulent equivalent of ν and is commonly known as the turbulent eddy viscosity.

In the present model the eddy viscosity, ν_t, is written in terms of the turbulent kinetic energy k and its dissipation rate ε:

$$\nu_t = c_\mu \frac{k^2}{\varepsilon} \tag{5}$$

where c_μ is a universal constant with a value of $c_\mu = 0.09$.

The kinetic energy, k, and its dissipation rate, ε, are solved from two partial differential equations in k and ε, both containing ν_t, and referred to as energy transport equations. For a detailed description of these equations for the standard k-ε model, see Rodi (1980).

2.2 Boundary Conditions

In the present model the the law of the wall is used at the bed:

$$\frac{u_t}{u_*} = \frac{1}{\kappa} \ln \frac{y_1}{y_0} \tag{6}$$

where:

u_t = the tangential velocity at a distance y_1, which is the distance of the first grid line, from the bed,

u_* = the shear velocity

κ = the von Karman constant

y_0 = $r_N/33$ with r_N being the equivalent Nikuradse roughness length

The following boundary conditions are used with respect to the bed in the equations of the k-ε model:

$$k = \frac{u_*^2}{\sqrt{c_\mu}} \tag{8}$$

$$\varepsilon = \frac{|u_*|^3}{\kappa y} \tag{9}$$

At the upstream boundary the standard distribution functions for uniform open channel flow are applied with regard to u, v, k and ε.

A rigid lid is applied along the free surface. The pressure distribution against the lid, which in fact is a fixed boundary without shear, acts on the fluid similarly to the pressure resulting from the free surface elevations, see Alfrink (1982).

2.3 Sediment Concentration Field

A spatial distribution of sediment exists as a result of the exchange of sediment between the flow field and the bed and due to further vertical exchanges caused by flow turbulence. Due to gravity forces acting on the grains the sediment concentration, in general, tends to increase towards the bed. In the present model the variation in bottom topography is found using the computed flow field.

The following unsteady equation describing the conservation of sediment is used in the model to derive the bottom boundary condition:

$$\frac{\partial c}{\partial t} + u \frac{\partial c}{\partial x} + (v - v_s) \frac{\partial c}{\partial y} - \frac{\partial}{\partial x} (D_x \frac{\partial c}{\partial x}) - \frac{\partial}{\partial y} (D_y \frac{\partial c}{\partial y}) = 0 \qquad (10)$$

where:

c   =   the sediment concentration
v_s =   the fall velocity of the sediment in still water
D_x and D_y =   the coefficients of sediment diffusion in the x and y direction respectively

Combining Eq. (10) with the equation for continuity, Eq. (2), it follows that:

$$\frac{\partial c}{\partial t} + \frac{\partial}{\partial x} \left(uc - D_x \frac{\partial c}{\partial y} \right) + \frac{\partial}{\partial y} \left\{ (v - v_s) c - D_y \frac{\partial c}{\partial y} \right\} = 0 \qquad (11)$$

and that the horizontal and vertical transport through a unit area can be defined respectively as:

$$s_x = u \ c - D_x \frac{\partial c}{\partial y} \qquad (12)$$

$$s_y = (v - v_s) \ c - D_y \frac{\partial c}{\partial y} \qquad (13)$$

Boundary conditions with respect to the concentration field at the free surface (y = y_s) for the sediment and for the fluid are, respectively:

$$s_y = s_x \frac{\partial y_s}{\partial x} + c \frac{\partial y_s}{\partial t} \text{ and} \qquad (14)$$

$$v = u \frac{\partial y_s}{\partial x} + \frac{\partial y_s}{\partial t} \qquad (15)$$

leading, with Eqs. (12) and (13) to

$$v_s c + D_y \frac{\partial c}{\partial y} = D_x \frac{\partial c}{\partial y} \frac{\partial y}{\partial x} \qquad (16)$$

Similar boundary conditions apply for the bed (y = y_b) and assuming a constant porosity, p', for the bed thus leads to:

$$s_y = s_x \frac{\partial y_b}{\partial x} + c \frac{\partial y_b}{\partial t} - (1 - p') \frac{\partial y_b}{\partial t} \qquad (17)$$

$$v = u \frac{\partial y_b}{\partial x} + \frac{\partial y_b}{\partial t} \qquad (18)$$

$$v_s c + D_y \frac{\partial c}{\partial y} = (1 - p') \frac{\partial y_b}{\partial t} + D_x \frac{\partial c}{\partial y} \frac{\partial y_b}{\partial x} \qquad (19)$$

From Eq. (19) it is obvious that the term for vertical diffusion, which is in general negative near the bed, will hinder sedimentation.

Assuming that the coefficients of diffusion for water, v_t, (eddy viscosity) and for sediment, D_y, are equal, sedimentation will be hindered where the eddy viscosity field shows high values for v_t.
    Combining Eq. (11) for the concentration field with definitions of the horizontal and vertical transport, s_x and s_y, given in Eqs.

(12), (13), respectively, gives, after integration over the flow
depth, the equation of continuity of sediment

$$\int_{y=y_b}^{y=y_s} \left(\frac{\partial c}{\partial t} + \frac{\partial s_x}{\partial x} + \frac{\partial s_y}{\partial y}\right) dy = 0 \tag{20}$$

Using Eqs. (13), (16) and (17) leads to

$$\frac{\partial}{\partial t} \left(\int_{y_b}^{y_s} c \, dy\right) + \frac{\partial}{\partial x} \left(\int_{y_b}^{y_s} s_x \, dy\right) + (1-p') \frac{\partial y_b}{\partial t} = 0 \tag{21}$$

The total sediment transport capacity can now written as:

$$S = \int_{y_b}^{y_s} s_x \, dy \tag{22}$$

Using S according to Eq. (22) in Eq. (21) gives an alternative
formulation with regard to the bottom boundary condition for cases
where total sediment load is considered:

$$\frac{\partial}{\partial t} \left(\int_{y_b}^{y_s} c \, dy\right) + \frac{\partial S}{\partial x} + (1-p') \frac{\partial y_b}{\partial t} = 0 \tag{23}$$

For the computation of the bottom changes use has been made of
Eq. (23) assuming a stationary concentration field ($\partial/\partial t = 0$). The
objective of the study is to analyze the evolution of scour beneath a
pipeline. The bottom changes will be restricted to the characteristics
of bottom changes due to bed load.

2.4   Bed Load Transport

For cases with bed load transport a suitable bed load transport
formula is used to compute S. The transport capacity S is calculated
using the computed bed shear u_* and the threshold value u_{*c}. The value
of u_{*c}, indicating the initiation of bed load transport, has been
determined experimentally by many investigators, for instance Shields
(1936). In the course of this study three bed load formulae will be
considered. The first formula is similar to the Meyer-Peter Müller
formula:

$$\Phi = a \, (\theta - \gamma_s \, \theta_c)^b \tag{24}$$

where

$$\Phi = \frac{S}{(g\Delta D^3)^{\frac{1}{2}}} \text{ and } \theta = \frac{u_*^2}{\Delta g D} \tag{25}$$

The values of the parameters a and b have been chosen 13.3 and
1.5 respectively. The parameter γ_s represents the influence of the
local bed slope dy_b/dx on the threshold value u_{*c} and is defined,
using ψ the angle of internal friction of the sediment, as:

$$\gamma_s = \sin\{\psi - \text{arctg}(dy_b/dx)\} \ (\sin\psi)^{-1} \tag{27}$$

An example of an empirical formula describing in particular conditions with minor sediment transport is the formula of Paintal (1971):
$$\Phi = 6.56 * 10^{18} \ \theta^{16} \tag{28}$$

De Ruyter (1982) has elaborated upon the stochastic description of sediment transport. He has expressed the sediment transport rate as a function of the pick up rate N_p and the saltation length λ. In dimensionless terms this formula can be expressed as:

$$\Phi = \Pi \ \Lambda \tag{29}$$

where

$$\Pi = \frac{\pi D^3}{6} \ \frac{N_p}{\sqrt{\Delta g D}} \ \text{and} \ \Lambda = \frac{\lambda}{D} \tag{30}$$

The formula of N_p is given in the Appendix by (A3). An important parameter is the dimensionless saltation length $\lambda/D = a' \ \theta$. For $\theta \leqslant \theta_c$ it has been assumed that a' approaches $550 \ \theta_c/\theta$. For $\theta > \theta_{cr}$ the value of a' has been assumed to be equal to 550. The ratio of σ_τ/τ and θ_c have been estimated at a value of 0.4 and 0.1 respectively. It should be emphasized that the transport rate described by (A1) has been reduced with a factor of 3 for calibration purposes.
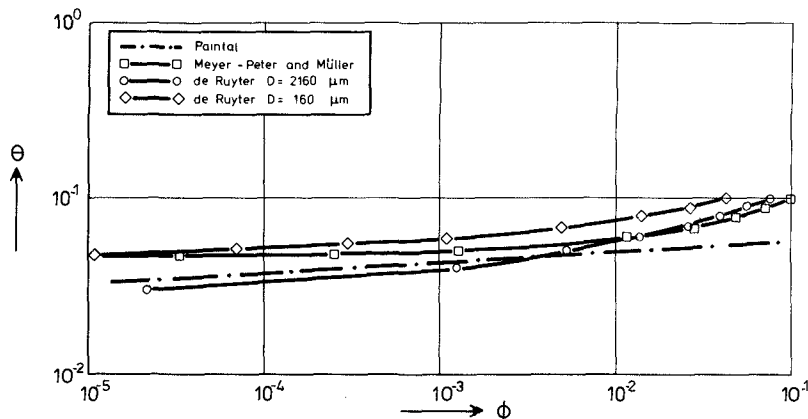
FIG. 2 COMPARISON OF BED LOAD TRANSPORT FORMULAE

The tendency of all the transport rates in Fig. 2 is similar, i.e. a rapid decrease in transport rate near the ciritcal Shields value. This implies that for a given shear stress distribution, the transport distributions for the presented transport formulae will also be similar of shape even as the resulting bottom changes. This conclusion will be used in the analysis of the scour underneath the pipe. Finally it may be remarked that although the shape of the bottom changes is similar, the magnitude depends among others on the choice of the transport formula.

3. Examples

    As an example has been chosen the scour beneath a submarine pipe-
line. Characteristic features of the scour hole obtained from labora-
tory experiments can be found in Figs. 3 and 4. First the equilibrium
scour hole will be treated followed by the evolution of a scour hole
with time.
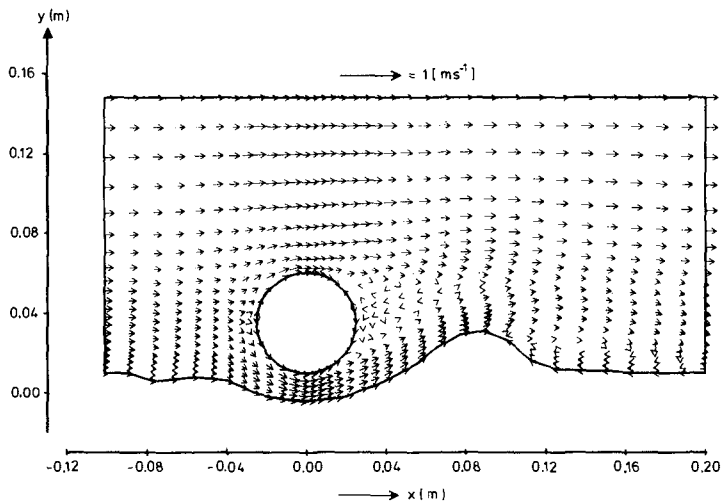
FIG. 3a   FLOW PATTERN
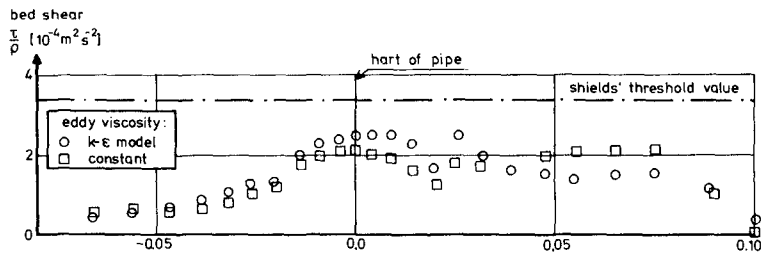
FIG. 3b   COMPUTED BEDSHEAR
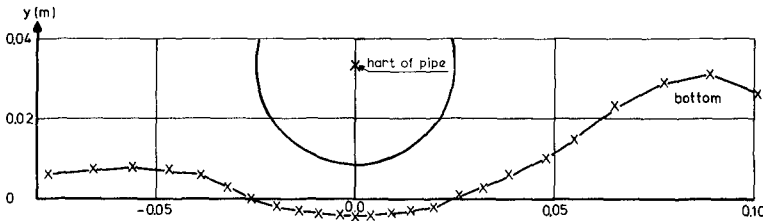
FIG. 3c   CONFIGURATION OF SCOURHOLE

3.1   Equilibrium Scour Hole

     The bed shear has been computed along the bottom of a scour hole
for a situation with clear water scour, when the sediment supply
towards the area of scour is zero. Although minor movement of indi-
vidual grains was observed occasionally in the small scale scour test
in the laboratory the scour hole can be assumed to show its equilib-
rium shape. The minor grain movement occurred on the rising slope and
was due to fluctuations in the bed shear. The flow field is shown in
Fig. 3a. Fig. 3b shows the computed bed shear for a constant viscosity
of 10^{-4} [$m^2 s^{-1}$] and also for an eddy viscosity computed by the k-ε
model. The computed time mean bed shear downstream of the pipe is a
little below Shields' mean threshold value which is approximately
$u_*^2/(\Delta gD) = 0.03$ for the grain diameter used in the test. This is in
agreement with the observation that the scour hole is in an equilib-
rium state. The test data of the example are:
-   pipe diameter   :   50 mm,
-   mean current velocity: 0.25 ms^{-1}
-   grain size   : D_{50} = 700 μm
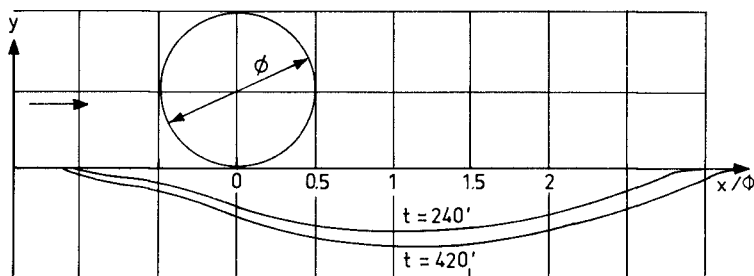
FIG. 4a SCOUR EVOLUTION
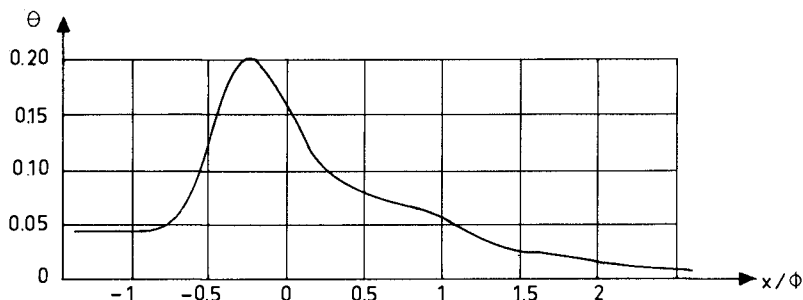

FIG. 4b COMPUTED BED SHEAR

3.2   Scour Development with Time

In this example the evolution of the scour hole has been computed starting with the geometry of a partially developed scour hole.
Five morphological time steps have been made each preceeded by a series of hydraulic time steps, covering a total time interval of 5 minutes of the scour process. The computed bed shear is shown in Figs. 4a and 4b together with scour hole configurations as observed during the small-scale test after 240 and 420 minutes scouring respectively. Fig. 4a shows the further evolution of the scour hole, during the 5 minutes after t = 420 minutes, as computed using the bed load concept of the model.

A propagating bed wave or ripple appears as a direct consequence of the use of a transport formulation relating the bed load transport to the bed shear. Its propagation velocity, c_b, is approximately 0.36 [m/hour] and the height of the crest, Δ_{bt}, and the depth of the trough, Δ_{bd}, converge to values of 0.014 and 0.007 m respectively, see Fig. 5b. Because of the persistence of the ripple the computations have been terminated after 5 minutes. In order to analyse these bed


time step:
$\Delta t_m \simeq 1'$
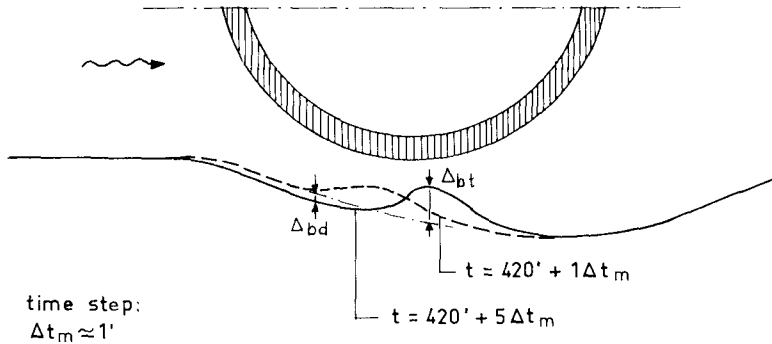
FIG. 5a   COMPUTED EVOLUTION OF SCOUR HOLE DUE TO BED LOAD TRANSPORT
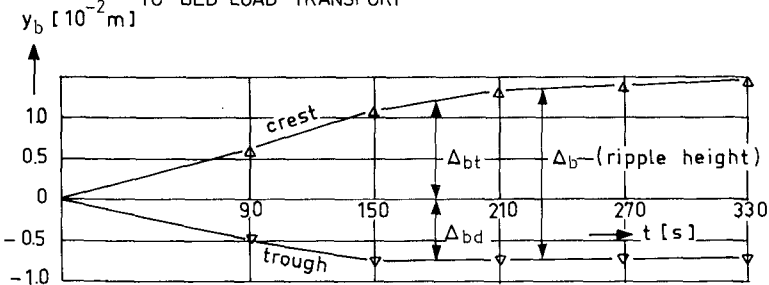
FIG. 5b RIPPLE DEVELOPMENT RELATIVE TO LOCAL INITIAL BED

features the computed sediment transport, S_b, is given in Fig. 6a
together with the mean sediment transport, S_m, during the 3 hour time
interval between the two scour hole configurations shown in Fig. 4a.
It will be clear from Fig. 6a that the computed bed load transport
capacity at t = 420 deviates considerably from the mean value computed
over the three hourst time preceding t = 420. In Section 4 this dis-
crepancy will be further analyzed.

    The test data are:
-   pipe diameter   :   140 mm,
-   mean current velocity: 0.40 ms^{-1},
-   grain size   : D_{50} = 100 [µm]

sediment transport
capacity [10^{-6} m^3 s^{-1}m^{-1}]
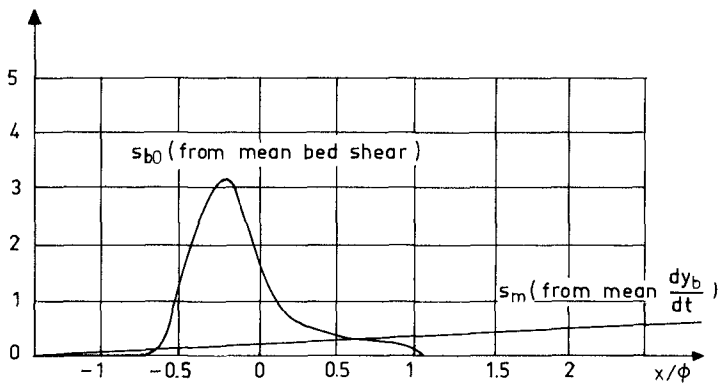
FIG. 6a COMPUTED AND OBSERVED SEDIMENT
         TRANSPORT DISTRIBUTIONS

gradient of transport [ms^{-1}]
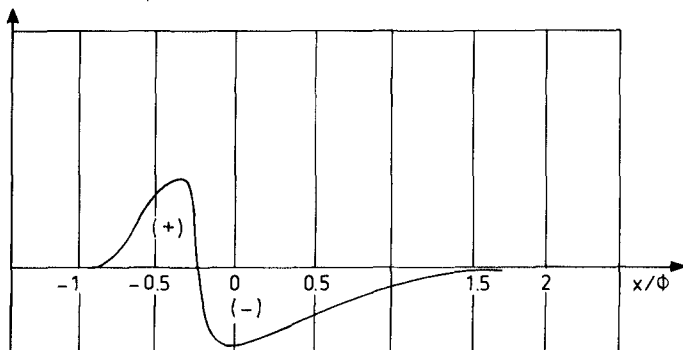
FIG. 6b COMPUTED SEDIMENT TRANSPORT GRADIENTS

4. Analysis at the Results and Discussion

     In view of the results in the examples treated in Sections 3.1
and 3.2 a first assessment can be made of the role that can be
ascribed to bed shear with regard to local seabed morphology.
     For the development and the equilibrium state of scour underneath
submarine pipelines it can be assumed that the leading parameter is
the bed shear. An increasing scour depth can be assumed to be closely
related to an increasing bed shear in the direction of flow at least
for cases with dominating bed load transport. In line with this as-
sumption an equilibrium scour hole occurs when the bed shear remains
constant along the bed provided that the threshold value is exceeded.
     The example in Section 3.1 clearly confirms the assumption for an
equilibrium scour hole in coarse sediment where the sediment supply
upstream of the pipe equals zero. On the rising slope downstream it
was observed that minor movement of individual grains still occurred
even though the scour depth was practically in equilibrium. This ob-
servation is in agreement with the computed bed shear on the slope
which in the scour hole is nearly constant and just below the mean
threshold value of $\theta_c = u_{\ast c}^2/(\Delta g D) = 0.03$ according to Shields (1936).

     The example given in Section 3.2, in which the evolution of the
scour hole with time was treated, demonstrated the unsatisfactory de-
scription of the sediment transport given by formulae like Eq. (24),
even though bed load transport has been observed to contribute predo-
minantly to the scour development. The appearance of a wave in the bed
is inherent to the transport formulae like Eq. (24), where the sedi-
ment transport is so directly related to the bed shear. Fig. 6 clearly
demonstrates the reason for the bed wave or ripple developing in the
model. This reason is not numerical, but is a direct consequence of
the sediment transport concept chosen and the sign of $\partial S/\partial x$.

     During 5 minutes computing time the wave or ripple propagates in
the direction of the flow while a mean degradation of the bed is being
computed. All the sediment being transported by means of ripple propa-
gation, the net loss of sediment from the scour hole, is determined by
the propagation velocity and the height of the ripple.
     Fig. 4b indicates that the ripple converges to a certain height,
Δ_b, which may enable a computation of the time averaged loss of sedi-
ment using:

$$dA = \xi \, \Delta_b \, c_b \tag{31}$$

where
> dA =   the increase in scour volume per unit width and per unit
>   time and
> ξ =   a coefficient depending on the ripple configuration,
>   representing the effective ripple height.

     Using Eq. (31) with the computed values for c_b and the effective
ripple height $\xi \Delta_b$ the scour volume corresponding with the ripple pro-
pagation is of the same order as the observed mean scour from $t = 240'$
to $t = 420'$ (Fig. 4a).

     In the small-scale laboratory scour tests a gradual degradation

of the bed has been observed at the time interval of 180 minutes. In
the bed load concept a constant dy_b/dt means, that during that time,
$\partial s/\partial x$ is approximately constant and s increases gradually along the
bed in the direction of the flow (the theoretical curve s_m for the
transport capacity). Using the bed load concept the computed transport
confirms with the curve s_b which in turn conforms to the bed shear in
Fig. 3b. Both curves for the transport deviate considerably, indica-
ting that the concept of bed load as a direct function of the time
averaged bed shear is not unconditionally sufficient to describe local
scour. Four reasons for this insufficiency are discussed below. These
reasons are a) suspended transport, b) stochastic bed shear, c) bed-
form roughness and d) transport formulation.

a)   Suspended transport
      It is obvious that with increasing bed shear sediment will be
brought into suspension and a concentration field will develop result-
ing in additional convective and diffusive sediment transport in addi-
tion to the bed load transport. Ripples, appearing as a result of
strong bed shear gradients as shown in the example, will, in the very
initial phase, be in suspension. Suspended sediment transport will be
included in a more extended version of the present program and will be
based upon the equations given in Par. 2.3.

b)   Introduction of stochastic bed shear
      In turbulent flow the bed shear has a stochastic character and
consists of a constant time averaged value τ, which follows directly
from the present model, and a fluctuating component τ'. Using only
τ for the computation of the bed load transport capacity according to
Eq. (24) the contributions of instantaneous bed shear values τ (or u_*)
with a probability $p(\tau)$, or $p(u_*)$, can be neglected.
      Instantaneous values of $\tau > \tau$, even though their probability may be
low, can contribute considerably to the sediment transport capacity.

      Laboratory measurements have demonstrated that the significant
turbulence downstream of pipelines which can be practically expressed
in standard deviations, σ_u, of the flow velocity.
      Once the turbulent kinetic energy, k, is known and assuming $v' \ll$
u' the standard deviation σ_u follows from:

$$\sigma_u = \sqrt{2k} \qquad\qquad\qquad (32)$$

      In the appendix a method is given which, starting with σ_u,
through σ_τ results in an amplification factor, A, for the sediment
transport capacity. A is a function of the mean bed shear level, β,
and the relative level of turbulence, α/α_o. By multiplying the sedi-
ment transport capacity, S_{bo} and using only the mean bed shear
τ (or $\bar{u}_*$), by A the sediment transport capacity, S_b is obtained which
also includes the effect of variation of turbulence. In case of $\tau < \tau_c$
the Meyer-Peter Müller formula (24) yields a zero transport rate inde-
pendent of the variation of turbulence. Fig. 7 shows A as a function
of α/α_o and β and is further explained in the Appendix. Fig. 8 shows
the effect of the measured relative turbulence, α/α_o, for the pipeline
example discussed in Section 3.2. Above $x/\emptyset = 1.0$ the computed ampli-
fication factor increases rapidly due to the low bed shear level,
$\beta = \tau/\tau_c$, (see Fig. 7), and, finally, β arrives at values where the

approach leading to a value of the amplification factor is no longer
applicable.
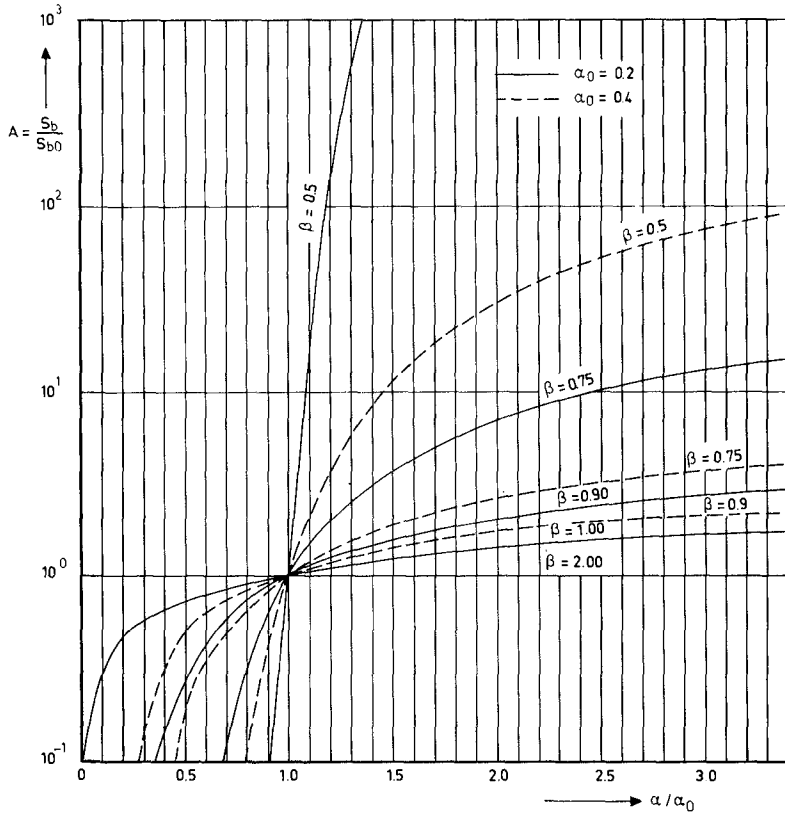
FIG. 7 AMPLIFICATION OF SEDIMENT TRANSPORT AS A FUNCTION
        OF SHEAR STRESS LEVEL β , AND RELATIVE
        TURBULENCE INTENSITY α/α_0

    According to Fig. 8 the amplification factor beneath the pipe is
one. This means that introduction of stochastic bed shear does not
influence the ripple height. On the lee side locally the amplification
factor increases rapidly (Fig. 8). This increase is caused partly by
the decrease in S_{bo} in Eq. (A6). Due to the local effect in the
present example it is not expected that introduction of stochastic bed
shear will in this case lead to a more uniform erosion on the lee side
of the pipe.

c) Varying bed roughness
    In the small-scale scour tests with movable bed it has been ob-
served that, in general, the bed becomes smooth underneath the pipe
and that the ripple pattern is restarted on the downstream slope.

Although this phenomenon will be less pronounced for larger scale
scour its influence on the bed shear, Eq. (6), and the related trans-
port (mechanism) should be taken into account.
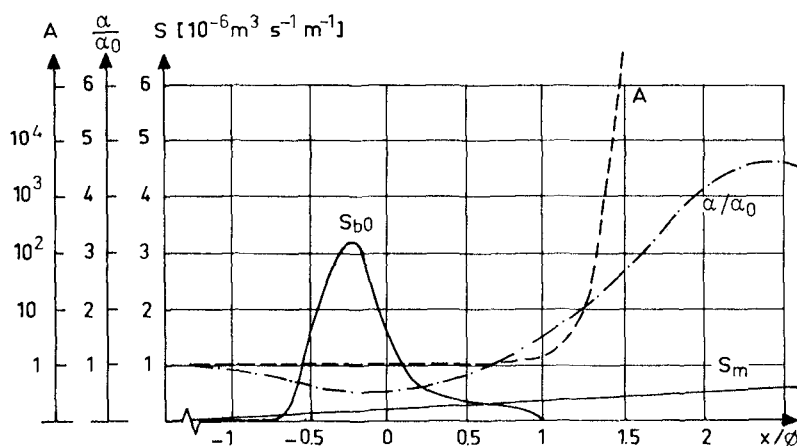
FIG. 8 OBSERVED TURBULENCE INTENSITY AND AMPLIFICATION FACTOR

d) Flexible transport formulation
     Relaxation of the rigidly formulated (bed load) formulae, Eq.
(24) and Eq. (28), by introducing variable coefficients a and b indeed
makes sense physically. It is known that the value of b, in particu-
lar, decreases when θ and, therefore, the transport, S, increases.
     The various influences on the redistribution of sediment trans-
port mechanisms underneath the pipe and downstream will without doubt
change the type of transport and its formulation.
     The use of a flexible formulation for the sediment transport,
though physically justified and even required, is not warrented at
present, because of lack of knowledge about the variation of the para-
meters.

5. Summary and Conclusions

     The local morphological changes beneath pipelines originating
from hydraulic conditions show variations which are on a relatively
small scale compared to the water depth. A numerical model to compute
these very local hydraulic conditions is essential for the study of
scour problems as for example can occur with a submarine pipeline. A
detailed computation of bed shear and turbulence characteristics, as
provided by the present model, has been used to obtain the sediment
transport capacity along the bed near a pipeline. Although the bed
shear is the leading parameter for the sediment transport a combina-
tion of the latter with an empirial bed load formula seems to result
in a rather rigid schematization of the complex sediment transport for
the presented examples of local scour. The computed bed changes in-
clude ripple development, at least when a bed load concept is used,

which excludes sediment suspending under the influence of high values
of local bed shear. The example with a computation on a flow field
around a pipe with an equilibrium scour hole has proved the value of
the present model for appreciating the morphological stability of
local seabed configurations.

Implementation of the suspended load concept is the next step
which will be taken in the further development of the present model.

6. Acknowledgements

The authors acknowledge the contributions of Mr. de Ruyter on
Fig. 2 and on the Appendix. Discussions with Dr. de Vriend and Mr. van
Rijn have appeared to be very fruitful.

7. References

ALFRINK, B.J., 1982: "Value of refined modelling for the flow over a
    trench". Proceedings of the International Symposium on Refined
    Modelling of Flows, Paris.
EINSTEIN, H.A., 1950: "The bed load function for sediment transporta-
    tion in open channel flows". Technical Bulletin No. 1026, U.S.
    Dept. of Agriculture, Washington D.C.
PAINTAL, A.S., 1971: "Concept of critical shear stress in loose
    boundary open channels". Journal of Hydraulic Research, No. 1
    91-107.
RODI, W., 1980: "Turbulence Models and their application in hydrau-
    lics". International Association for Hydraulic Research, Delft.
RUYTER, J.C.C. de, 1982: "The mechanics of sediment transport on bed
    forms". Euromech 156 Mechanics of Sediment Transport, Istanbul.
YALIN, M.S., 1977: "Mechanics of sediment transport". Oxford, Pergamon
    Press.

8. List of Symbols

A	amplification factor	[-]
a	coefficient transport formula	[-]
a'	coefficient saltation	[-]
b	coefficient transport formula	[-]
	index: bed	[-]
c	sediment concentration	[-]
	index: critical	[-]
c_b	propagation celerity of bed forms	[ms^{-1}]
c_μ	constant in k-ε model	[-]
D	grain diameter	[m]
D_x, D_y	coefficients of diffusion	[m^2s^{-1}]
dA	scour area	[m^2]
F	function symbol	[-]
g	acceleration of gravity	[ms^{-2}]
k	kinetic energy	[m^2s^{-2}]
N_p	pick-up rate	[s^{-1}]
p	pressure	[Nm^{-2}]
	probability	[-]
p'	porosity of sediment	[-]
r	excess bed shear	[-]
r_N	Nikuradse roughness	[m]

S	sediment transport capacity	$[m^2 s^{-1}]$
s	sediment transport capacity	$[ms^{-1}]$
t	time	$[s]$
u	velocity in x-direction	$[ms^{-1}]$
u_*	shear velocity	$[ms^{-1}]$
v	velocity in y-direction	$[ms^{-1}]$
v_s	fall velocity of grains	$[ms^{-1}]$
x	horizontal coordinate	$[m]$
y	vertical coordinate	$[m]$
y_b	bed level	$[m]$
y_s	water surface level	$[m]$
α	turbulence level, $\sigma_\tau/\bar{\tau}$	$[-]$
β	bed shear level, τ/τ_c	$[-]$
γ_s	slope factor	$[-]$
Δ	relative density of grains	$[-]$
Δ_b	ripple height	$[m]$
Δt	time step	$[s]$
ε	energy dissipation rate	$[m^2 s^{-3}]$
η	coefficient	$[-]$
θ	Shields bed shear parameter	$[-]$
κ	von Karman constant	$[-]$
λ	saltation length	$[m]$
ν_t	turbulent eddy viscosity	$[m^2 s^{-1}]$
ξ	coefficient	$[-]$
ρ	density of water	$[kgm^{-3}]$
σ_u	standard deviation of u	$[ms^{-1}]$
σ_τ	standard deviation of τ	$[Nm^{-2}]$
τ	(bed) shear	$[Nm^{-2}]$
$\emptyset$	pipe diameter	$[m]$
Φ	transport parameter	$[-]$
ψ	friction angle	$[-]$

APPENDIX: Increase of Bed Load Transport Capacity due to Turbulence

A method is described below to account for the effect of turbu-
lent fluctuations in the bed shear on the bed load transport capacity.
In general the instantaneous bed shear will contribute to the bed load
transport as soon as the threshold value, u_{*c}, (or correspondingly τ_c
or θ_c) is exceeded. The approach starts with a sediment transport for-
mulation based upon the displacement of an individual grain with dia-
meter D. Let N_p be the number of grains picked up by the flow per unit
of time and of the bed surface. Furthermore let λ be the saltation
length of a grains picked up by the flow. When the bed consists of
spheres with a volume of $1/6\pi D^3$, the bed load transport capacity can
be written as

$$S_b = \frac{1}{6} \pi D^3 N_p \lambda \qquad (A.1)$$

The saltation length is assumed to be proportional to both the
grain size, D, and the dimensionless bed shear, θ, for $\theta > \theta_c$, so that

$$\lambda = a' D \theta \qquad (A.2)$$

where a' is a dimensionless constant which, according to de Ruyter
(1982), has a value of a' $\simeq$ 300 to 800. In the computation the values
shown in Section 2 have been used.

According to Ruyter (1982) the pick-up rate, N_p, can be expressed
as

$$N_p = \frac{4\eta}{\pi D^2} \sqrt{\frac{\rho g \Delta \ tg\psi}{\rho_s D \tau_c}} \sqrt{\sigma_\tau} \ F_p(r) \qquad (A.3)$$

where
η = coefficient
$tg\psi$ = the friction coefficient for the grains
σ_τ = the standard deviation of bed shear
r   = $(\bar{\tau}-\tau_c)/\sigma_\tau$ a measure of the excess bed shear   (A.4)

$$F_p(r) = \frac{1}{\sqrt{2\pi}} \int_0^\infty \sqrt{x} \exp\{-\frac{1}{2}(x-r)^2\} \ dx \qquad (A.5)$$

The definition of the function, $F_p(r)$, originates from the as-
sumption that τ is Gaussian distributed with a mean $\bar{\tau}$ and a variance
σ_τ^2.

An amplification factor, A, can be defined as the ratio of the
bed load transport capacities, S_b and S_{bo}, both at the same mean bed
shear, $\bar{\tau}$, but with different fluctuations, σ_τ. Here S_{bo} is used as a
reference transport capacity at a "reference turbulence" $\sigma_{\tau o}$.
Combining Eqs. (A.3), (A.4) and (A.5) results in

$$A = \frac{S_b}{S_{bo}} = \sqrt{\frac{\sigma_\tau}{\sigma_{\tau o}}} \frac{F_p(r)}{F_p(r_o)} \qquad (A.6)$$

It is obvious that the relative change in bed load transport
capacity due to turbulence is a direct function of σ_τ and even though
the mean bed shear $\bar{\tau}$ remains constant, its absolute value has an

indirect effect through the function F_p. The actual value of the constant, a', in the formulation of the saltation length, λ, Eq. (A.2), appears to vanish in Eq. (A.6).

For any location along the bed the amplification factor, A, for the bed load transport can be found with Eq. (A.6) given a value for σ_τ. Assuming the instantaneous bed shear τ to be proportional to the square of the instantaneous velocity u near the bed one can express $\sigma_\tau/\bar{\tau}$ as:

$$\frac{\sigma_\tau}{\bar{\tau}} = \frac{\sigma_u}{\bar{u}} \frac{\sqrt{4+2(\sigma_u/\bar{u})^2}}{1+(\sigma_u/\bar{u})^2} \tag{A.7}$$

The variations, σ_u, of the total velocity u around its mean value $\bar{u}$ have been measured in a physical model but can also be derived from the turbulent kinetic energy, k, computed by the present model.

The influence of σ_τ on the bed load transport capacity can be shown conveniently by defining two parameters, α and β, which represent the levels of turbulence and mean bed shear respectively.

$$\bar{\tau} = \beta \, \tau_c \tag{A.8}$$

$$\sigma_\tau = \alpha \, \bar{\tau} \tag{A.9}$$

Combining Eqs. (A.8), (A.9) with Eq. (A.4) r is written as

$$r = \frac{\beta - 1}{\beta} \frac{1}{\alpha} \tag{A.10}$$

Given a value for r the value of $F_p(r)$ can be found numerically. The values of the amplification factor, A, according to Eq. (A.6), have been computed and plotted in Fig. 7 for various values for the relative turbulence α/α_0 and at a number of values for the bed shear level, β.

Values of 0.2 and 0.4 have been chosen as examples for the reference turbulence level, α_0. Measurements of the velocity upstream of the pipe at a distance of 0.01 m from the bed indicate $\sigma_u/\bar{u} \simeq 0.10$, leading, with Eq. (A.7), to $\sigma_\tau/\bar{\tau} = 0.2$. Most of the classical empirical (bed load) transport formulae originate from test conditions with uniform flow conditions with a turbulence $\sigma_\tau/\bar{\tau} \simeq 0.4$.

The bed load transport capacity computed with empirical formulae should, therefore, be amplified with a factor A using $\alpha_0 = 0.4$ as a reference and the actual mean bed shear as the bed shear level β.

The approach given here is limited practically by the extend of the function $F_p(r)$. For $r < -5$, $F_p(r)$ tends to approach zero. With Eq. (A.10) the limits can be indicated in terms of α_0 and β through $\beta = 1/(1+5\alpha_0)$.